❒   1714

One-dimensional Lumped-Circuit for Transient Thermal Study of an Induction Electric Motor

Radhia Jebahi, Helmi Aloui, Moez Ayadi
Laboratory of Advanced Electronic Systems and Sustainable Energy, University of Sfax, ENET'com, Sfax, Tunisia

Article Info	ABSTRACT

Electrical machines lifetime and performances could be improved when along the design process both electromagnetic and thermal behaviors are taken into account. Moreover, real time information about the device thermal state is necessary to an appropriate control with minimized losses. Models based on lumped parameter thermal circuits are: generic, rapid, accurate and qualified as a convenient solution for power systems. The purpose of the present paper is to validate a simulation platform intended for the prediction of the thermal state of an induction motor covering all operation regimes. To do so, in steady state, the proposed model is validated using finite element calculation and experimental records. Then, in an overload situation, obtained temperatures are compared to finite element's ones. It has been found that, in both regimes, simulation results are with closed proximity to finite element's ones and experimental records.

Corresponding Author:

Helmi Aloui,
Laboratory of Advanced Electronic Systems and Sustainable Energy,
National School of Electronics and Telecommunications (ENET'Com),
University of Sfax, ENET'Com, BP 1163, 3018 Sfax, Tunisia.
Email: helmi.aloui@enig.rnu.tn

1. INTRODUCTION

The energy conversion inside an electric machine leads inherently to the heat occurrence, essentially due to different proportions of iron and copper losses. In addition, an overheating of a motor is directly linked to the degradation of its performances [1-3]. Thus, in order to reduce such a limitation and avoid the damage of the device, it is necessary to gather the thermal analysis to the electromagnetic study during design process [3-5]. Indeed, the prediction of the temperature distribution in the different parts of the machine allows us to evaluate if the machine will reach the thermal class for which it is being designed and also to check if the supplied air flow of the cooling system is sufficient to a normal operation at rated conditions. Thereby, a satisfactory life span of the machine gathered to an improvement of its performances could be guaranteed. That explains the existence of several prediction methods of temperatures distribution inside electric motors, like: Computational Fluid Dynamics, Lumped Parameter Thermal Circuits, Finite Elements (FE) …, [6-10].

Thermal models based on lumped parameter were developed since a long time. In such models, each node represents a part of the machine and the thermal circuit, in the steady state, consists of thermal resistances and heat sources connected between motor components. For transient analysis, the heat capacitances are additionally used to take into account the ongoing changes. Despite the accuracy of this method, it needs several improvement. Indeed, in [11], the developed thermal model focused only stator parts. Whereas, when the permanent magnets (PM) are placed in rotor, it is necessary to expand the thermal model and take into account this part. In fact, PMs are very sensitive to the temperature rise and the choice of their polarization is directly related to their thermal behaviour. Moreover, in [12], the temperatures obtained by lumped parameter method were a little higher than the measured ones due to the hypothesis considered to elaborate the thermal model.

However, the originality of this paper consists of the development of a generic refined model giving thermal state of all parts of the machine, along all operation regimes, in an attempt to a future exploitation to develop a control strategy with minimum losses rates and to size appropriate cooling system. Presented works are applied on an induction motor and are organized as follows: the first part is devoted to the presentation of the developed lumped circuit for the thermal analysis of the considered device. Then, the second part is intended to the validation of the proposed model through a finite element calculation using a 2D model and also an experimental test, considering a steady state operation regime. Finally, the lumped circuit is exploited to predict the thermal state of the motor, when an overload regime is considered, and to compare obtained results to FE ones.

2.   THERMAL MODELING OF THE INDUCTION MOTOR

The present section is devoted to the description on the induction motor going to be studied and to the presentation of two thermal models. The first is based on lumped-circuit method and the second is intended to validate this latter through a finite element calculation.

2.1. Motor description

The induction motor is the ultimate industrial motor due to its robustness and affordable price, compared to the rest. Due to the hard constraints in industry, it is necessary to have an efficient tool telling about the thermal state of the machine, especially during overload or short-circuits situation, in order to guarantee equipment security and optimal control with reduced losses. Indeed, losses in electrical machines lead to the rise of the components temperatures which conducts to the degradation of their performances. Figure 1 shows the layout of the motor going to be modeled. It is a cage asynchronous motor with: pole pair number (2), voltage (220 V), power (0.37 kW), power factor (0.75), frequency (50 Hz), weight (63 kg), protection (IP55) and insulation class (F).

In order to prepare thermal modeling, the motor geometry is divided on layers as shown in Figure 2 and corresponding dimensions are measured, calculated and summarized in Table 1.
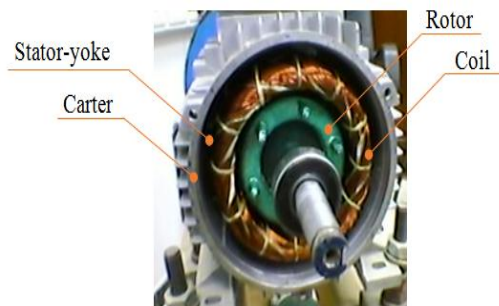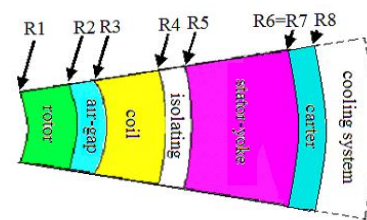

Figure 1. Layout of the studied motor

R1=6(mm), R2=33.1(mm), R3=33.2(mm), R4=48.2(mm), R5=48.5(mm), R6=R7=54.9(mm), R8=59.5(mm).

Figure 2. Layers distribution for thermal modeling of the motor

Table 1. Measured motor dimensions

Name	Value (mm)
Outer diameter rotor (R1)	12
Inner diameter of rotor (R2)	66.4
Air-gap thickness (e)	0.5
Inner diameter stator (R3)	66.5
Insulator height (hiso)	0.3
Stator yoke height (hcs)	6.45
Outer diameter of stator (R6)	109.8
Carter height (hca)	4.55
Active length (La)	89

2.2. Lumped-circuit of the motor

The 1D thermal modeling was used to integrate thermal aspects in the design of active and passive components in electronic circuits [13-16]. Thanks to the simplicity and efficiency of this technique, it becomes increasingly used for the analysis of thermal behavior of electric machine [12], [17], [18].

Thermal models based on lumped-circuit method are built using thermal-electrical analogy. Indeed, this technique represents the thermal problems by the development of an electrical equivalent circuit using resistances and thermal capacitances [16-19]. Depending on the kind of thermal exchange, we can distinguish two types of thermal resistance: the conduction thermal resistance and the convection thermal resistance. In steady state, the thermal circuit is a network consisting of thermal resistances and heat sources connected between nodes representing motor components. Besides, for transient analysis, thermal capacitances are additionally inserted to take into account the ongoing internal energy changes.

The general expressions of the conduction thermal resistance (Rcond) and one of the convection thermal resistance (Rconv) are respectively given by Equations (1) and (2).

$$R_{cond} = \frac{e}{\lambda S} \tag{1}$$

$$R_{conv} = \frac{1}{h S_c} \tag{2}$$

Where: e is the distance between the point masses, S is the interface area, λ is the heat conductivity, Sc is the cooling cross section between the two regions and h is the convection coefficient calculated from proven empirical dimensionless analysis algorithms.

In addition, the thermal capacitance represents the ability of a component to absorb heat and is generally expressed as in Equation (3).

$$C = V \rho c \tag{3}$$

Where: V is the volume, ρ is the density and c is the heat capacity of the material.

In different works [11], [17], the thermal studies were based on limited models focused only on stator components. However, we propose in this paper a 1D thermal model, Figure 3, allowing us to have real time information about happening temperature's changes in different motor components. In this model, each component is represented by thermal resistances Ri and thermal capacitances Ci whereas heat sources correspond to copper and iron losses.

Since the structure of the induction motor is cylindrical, the thermal resistances of the different parts of motor are calculated after the resolution of the heat transfer Equation (4) in the radial direction.

$$-\lambda \, \nabla^2 T + \rho c_p \frac{\partial T}{\partial t} = \dot{q} \tag{4}$$

Taking into account the boundary conditions, the heat sources, and motor dimensions given in Figure 2 and Table 1, the thermal resistances and capacitances of the proposed model are expressed as in the following Equations. Calculated values of those resistances and capacities are summarized in Table 2.

- Rotor

$$R_{rotor} = \frac{1}{4\pi L \lambda_{\text{rotor}}} \left(1 - 2 \frac{R_1^2}{R_2^2 - R_1^2} \ln \frac{R_2}{R_1} \right) \tag{5}$$

$$C_{rotor} = V_{rotor} \, \rho_{rotor} \, c_{rotor} \tag{6}$$

- Coil

$$R_{coil} = \frac{1}{4\pi L \lambda_{\text{coil}}} \left(1 - 2 \frac{R_3^2}{R_4^2 - R_3^2} \ln \frac{R_4}{R_3} \right) \tag{7}$$

$$C_{\text{coil}} = V_{\text{coil}} \, \rho_{\text{coil}} \, c_{\text{coil}} \tag{8}$$

- Insulator

$$R_{iso} = \frac{\ln \frac{R_5}{R_4}}{2\pi L \lambda_{\text{iso}}} \tag{9}$$

$$C_{\text{iso}} = V_{\text{iso}} \, \rho_{\text{iso}} \, c_{\text{iso}} \tag{10}$$

- Stator-yoke

$$R_{yo} = \frac{1}{4\pi L \lambda_{yo}} \left(1 - 2 \frac{R_5^2}{R_6^2 - R_5^2} \ln \frac{R_6}{R_5} \right) \qquad (11)$$

$$C_{yo} = V_{yo} \, \rho_{yo} \, c_{yo} \qquad (12)$$

- Carter

$$R_{ca} = \frac{\ln \frac{R_8}{R_7}}{2\pi L \lambda_{ca}} \qquad (13)$$

$$C_{ca} = V_{ca} \, \rho_{ca} \, c_{ca} \qquad (14)$$

Table 2. Calculated values of resistances and thermal capacity

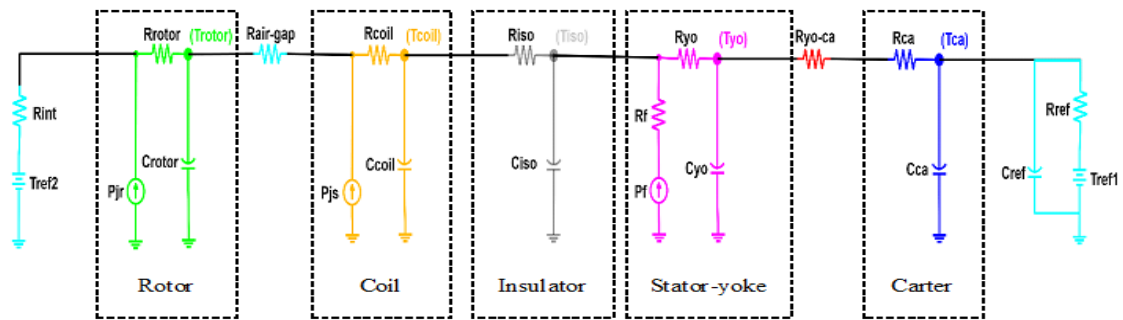| Motor components	Rotor	Coil	Insulator	Stator-yoke	Carter
Thermal resistance (W/K)	0.0062	0.0012	0.068	0.0049	0.0011
Thermal capacity (J/K)	454.2773	43.3026	7.634	920.1224	221.6182

Figure 3. 1D Thermal model of the motor implemented on Matlab-Simulink

2.3. Finite element model of the motor

The finite element method is used for numerical analysis of engineering problems (Mechanical, Electromagnetic, Thermal, Biomechanics, etc.) to obtain approximate solutions with very satisfying accuracy and closed proximity to the reality. This technique is increasingly being employed in the thermal analysis of electrical machines [7], [8], [17]. Several software platforms are devoted for this kind of calculations as long as the study domain is defined around specific model and boundary conditions.

In the present case, the motor is supposed to be thermally isotropic along active length direction. Thus, a 2D finite element model is sufficient to carry out the motor thermal state for any operation regime. Figure 4 shows the 2D study domain, the cooling system is modeled as a forced convection through the boundary condition (a) and the temperature rise in air-gap caused by the copper losses in rotor is taken into account as a boundary condition (b). In addition, Table 3 shows the thermal proprieties of motor components materials.

2.4. Simulation results and discussion

At this stage, we are interested in the comparison of temperature evolutions inside the motor obtained respectively by the lumped circuit and the FE model for both a static study and a transient one.

2.4.1. Static analysis

The static study is conducted in an attempt to focus the maximal temperature that could be reached in each element of the motor. Such a temperature is obtained when steady-state is reached, after a calculation time of 4200 s. In fact, we illustrated in Figure 5 the evolution of temperature inside the motor armature. On this figure we can see that, at the starting point the temperature is uniform and equal to the ambient

temperature (a). Then, after few operating seconds, the obtained distribution is illustrated in (b). These temperatures rise gradually according to the node's position to reach finally the steady-state (c), where the temperature is maximal and uniform.

As an illustration, Figure 6 shows the temperature evolution of the stator coil (a) and the stator yoke (b) versus the stator copper losses carried out using lumped-circuit (1) and FE model (2). Shown results are the extrapolation of the three marked points in the mentioned figure, corresponding to an average ambient temperature of 29 °C and the calculation conditions itemized in Table 4. We can remark the total harmony between lumped-circuit values and FE ones.

Table 3. Thermal properties of the motor's materials

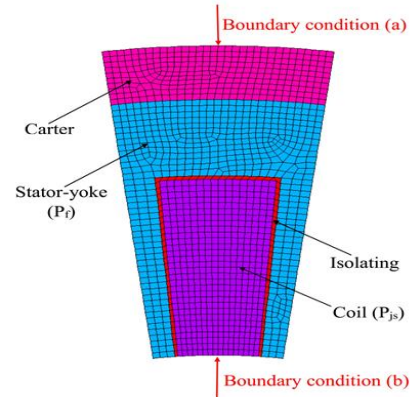| Material	Copper (Coil)	Insulator	Iron (Stator-yoke)	Aluminum (Carter)
Conductivities (W.m-1.K-1)	386	25	73	204
Mass heat capacity (J.kg-1.K-1)	383	1250	452	896
Density (Kg.m-3)	8954	1200	7870	2707

Figure 4. Meshed 2D finite element thermal model

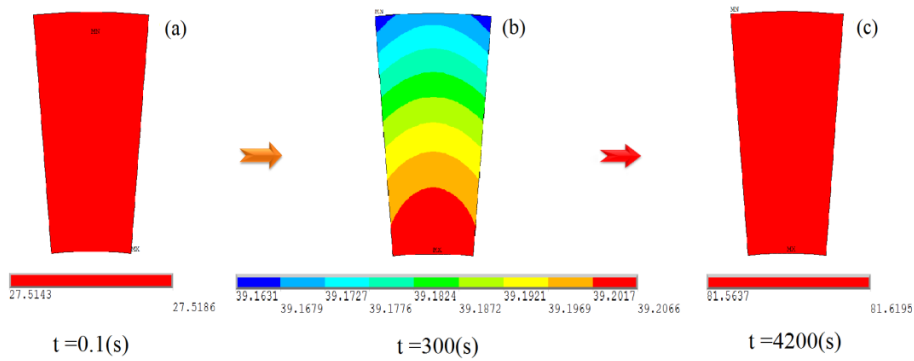t =0.1(s)   t =300(s)   t =4200(s)

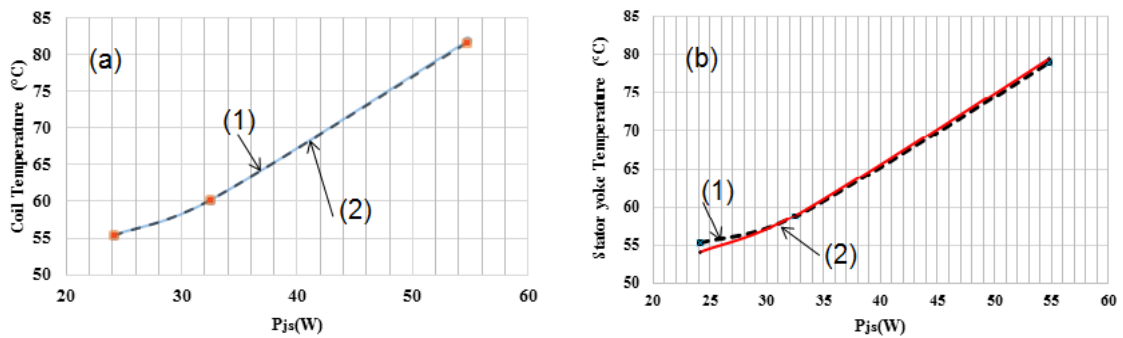Figure 5. Temperature distribution in stator coil

Figure 6. Evolution of the stator coil temperature (a) and the stator yoke temperature (b) versus the stator copper losses. Legend: (1): Lumped-circuit results and (2): FE results

Table 4. Simulation conditions of the static study

Conditions	Point 1	Point 2	Point 3
Iron losses (w)	26.5	26.5	26.5
Stator copper losses (w)	24.1	32.5	25.79
Rotor copper losses (w)	0	25.79	44.2

2.4.2. Transient analysis

In order to prove the accuracy the developed lumped-circuit, the thermal state of the motor is carried out in transient regime as shown in Figure 7 for the motor's armature. Results are obtained for when the following conditions are considered: ambient temperature: 28.2 °C, iron losses: 26,5W, stator copper losses: 32.45W and rotor copper losses: 25.79 W. A good accuracy is noticed between the lumped-circuit values and the FE ones where the introduced error does not exceed 5% in the worst case. Moreover, it is to be signaled that, from the point of view of simulation cost, the 1D thermal model is extremely fast compared to the FE one: A CPU-cost ratio of (104) is registered between the two simulations when they are performed with a Pentium processor. Thus, the lumped-circuit could be convenient solution to satisfy control requirement consisting of real time information about happening temperature's changes in different motor components.

3. EXPERIMENTAL VALIDATION

As mentioned previously, our purpose is to establish a simulation platform prediction of the thermal state of an induction motor covering all operation regimes. To do so and before expanding our works to other régimes, we intend in the present section to validate experimentally previous presented models (lumped-circuit and FE model).

Two tests are performed: at no-load then and under load operation regimes, considering the conditions given in Table 5 and using the built test bench of Figure 8 composed of:

a. The induction motor: on which thermal measurement are performed
b. An autotransformer: gradual star of the induction motor
c. The motor load: A coupled DC generator feeding a resistive load
d. A digital power meter: measurement of electrical magnitudes (power, current and voltage)
e. An infrared thermometer: to pick up the temperature in each component of the motor, where: Xr is the measurement point on the rotor, Xco is the measurement point on the armature, Xsy is the measurement point on the stator yoke and (Xca1 and Xca2) are two symmetric measurement points on the carter. In addition, in order to have access to the internal parts, two apertures are made in the motor carter. The first one, (1), serves for the temperatures of coil and stator-yoke, while the second, (2), is used for the rotor's temperature, Figure 8.

At this stage, it is to be mentioned that each experimental lasts for 4200 seconds and the temperature of each element is measured every minute.
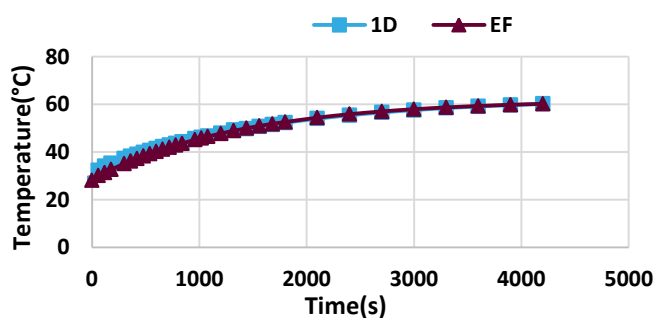

Figure 7. Evolutions of the stator coil temperature

Table 5. Energetic conditions of experimental tests

| | No-load operation | Load operation | |
		100(W)	400(W)
I(A)	1.06	1.23	1.598
P_f(W)	26.5	26.5	26.5
P_{js}(W)	24.1	32.45	55.774
P_{jr}(W)	0	25.76 9	44.208

3.1. No-load operation study

The energetic state of the motor corresponding to the no-load operation test is given in Table 5.

The evolutions of the picked temperatures in the carter symmetric points (Xca1 and Xca2) are illustrated in Figure 9. We can observe that the temperature is uniform both point which permits to verify the symmetry hypothesis used to elaborate the 1D thermal model and the FE one.

Furthermore, Figure 10 and Table 6 show a good accuracy between the experimental measurements of the coil temperature and its values obtained by the 1D thermal and the finite element models with an error less than 2.75%.
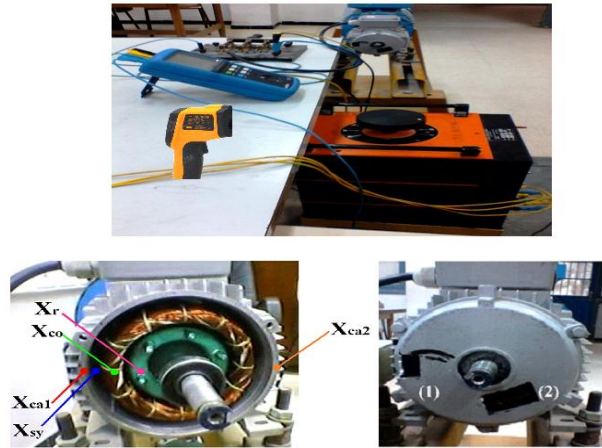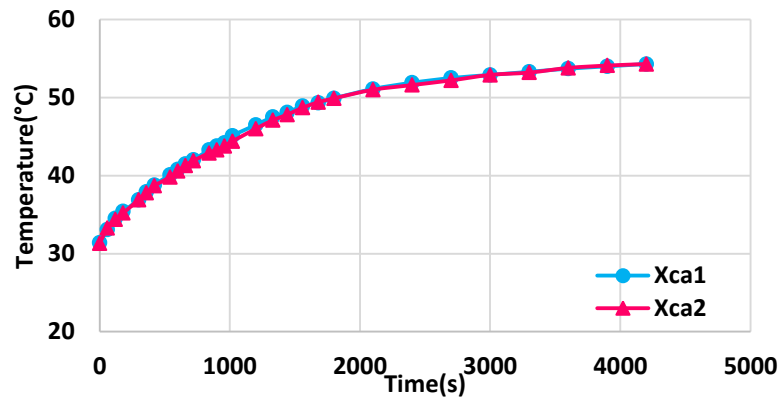

Figure 8. Experimental test bench

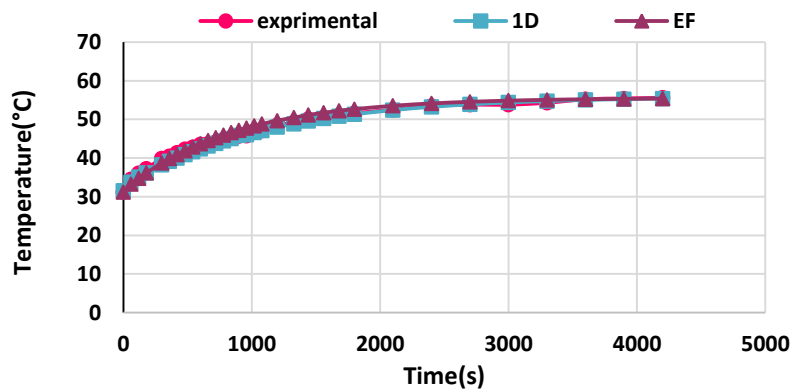Figure 9. Evolutions of the temperatures in carter under no-load operation

Figure 10. Evolutions of the coil temperature during no-load operation

3.2. Load operation study

The energetic state of the motor corresponding to the present test is given in Table 5.

Figure 11 shows the evolutions of the armature temperature picked experimentally and evaluated using the lumped-circuit and the FE model considering two values for the load connected to the DC generator (100 W and 400 W). Referring to such figure and also to Table 7, we can notice a high accuracy between the experimental measurements of the coil temperature and its values obtained by the 1D thermal and the finite element models with an error less than 2.7%.

Table 6. Comparison results (No-load operation)

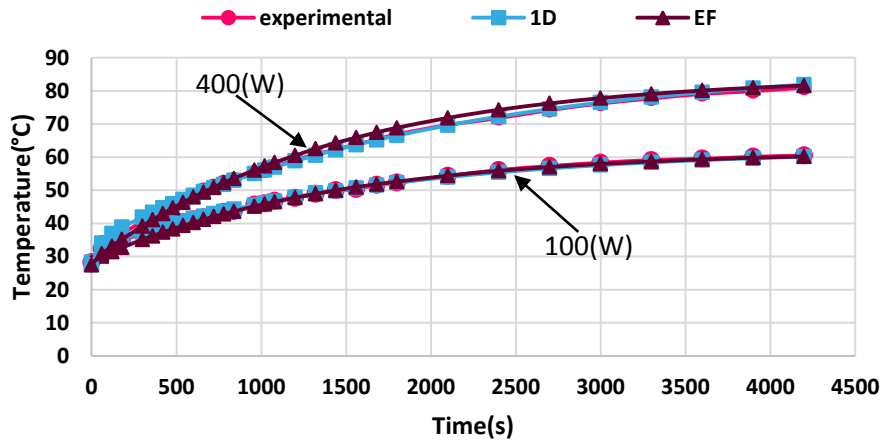| Time (s)	Measured temperature	1D	EF	Error % 1D	Error % EF
540	42.8	41.63	42.83	2.73	0.07
720	44.1	43.16	45.25	0.77	2.6
780	44.8	44.4	45.95	0.89	2.5
1320	49.2	48.83	50.46	0.75	2.5
2700	53.8	53.88	54.44	0.14	1.3
3600	55.2	55.03	55.2	0.3	0
3900	55.4	55.24	55.31	0.28	0.16
4200	55.6	55.41	55.38	0.34	0.39

Figure 11. Evolutions of the coil temperature during load operation

Table 7. Comparison results (Load operation)

Time (s)	100(W) Measured temperature	1D	EF	Error % 1D	Error % EF	400(W) Measured temperature	1D	EF	Error % 1D	Error % EF
540	40.4	40.67	39.32	0.6	2.6	46.6	47.2	46.3	1.28	0.64
720	42.5	42.91	42.02	0.96	1.12	51.1	50.75	50.88	0.68	0.43
780	43.4	43.61	42.85	0.48	1.2	52.3	51.75	52.28	1.05	0.03
1320	48.9	49.18	48.91	0.5	0.02	60.8	60.55	62.5	0.4	2.7
2700	57.3	56.59	57.02	1.23	0.48	74.2	74.51	76.2	0.41	2.69
3600	59.5	59.11	59.3	0.67	0.3	79.1	79.59	80.1	0.61	1.27
3900	60.1	59.68	59.81	0.69	0.48	79.9	80.83	80.94	1.6	1.3
4200	60.5	60.16	60.2	0.56	0.49	81	81.9	81.6	1.1	0.7

All performed tests, at no-load and under load regimes, prove a high satisfactory accuracy level between thermal states of the induction motor obtained through experimental measurement and carried out using the established models (lumped-circuit and FE model). Consequently, we can qualify both models as valid tools to be used for the exploration of the thermal state of the motor, especially when experimentation is either difficult to implement or harmful as in overload operation regimes like short-circuits under nominal voltage supply.

4.   OVERLOAD OPERATION

The motor components are subjected to the load and temperatures variations according to the operating cycle and ambient conditions. They are stressed heavily due to the effects of temperature cycle and face to the overheating risk that can cause the degradation of the motor performances and a raise of losses which must be kept below critical values during all operation regime. In fact, a raise of temperature level caused by an overload operation changes coils parameters (resistance and inductance) which leads to wrong control instructions in numerous strategies where such parameters are considered fix. Figure 12, shows the evolution of the armature's resistance versus the temperature of the studied induction motor, using Equation (15).

$$R(T) = R(T_0) * \{1 + \alpha * (T - T_0)\} \tag{15}$$

Where:
   a.   R (T): the resistance at the temperature T
   b.   R (T0): the armature resistance at the ambient temperature T0. In the present case, R(T0) has been measured at T0=29.9°C and was equal to =14.3Ω.
   c.   α: the temperature coefficient (α=3.9*10^{-3} C^{-1})

Inconvenient control orders are the origin of several phenomena limiting the device lifetime like vibration and mechanical fatigue. Thus, a predictive rapid model providing real-time information about the thermal state of the motor with acceptable accuracy could be a good solution permitting to perform advanced and complete control schemes taking into account the evolution of the machine parameters and the prevention of damages. For this reason, it is necessary to consider a coupled problem based on an electromagnetic model, for losses quantification, and an electro-thermal one in order to carry out real-time information about the thermal state of the motor with acceptable accuracy leading to adjusted d-q control currents, Figure 13.
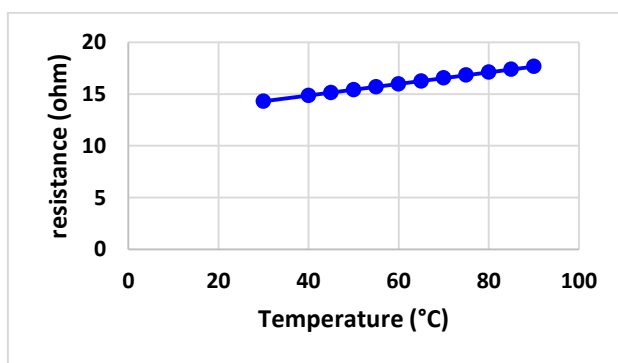
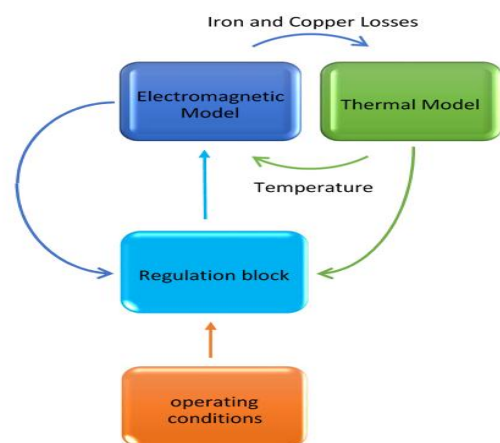Figure 12. Coil resistance versus motor temperature

Figure 13. Control algorithm

The present work focuses the electro-thermal part of the coupled problem by the establishment of a refined lumped circuit giving accurate results, as proved previously through the comparison with FE values and experimental records. Now, we are going to test the ability of such model to detect sudden variation of

the coil temperature when an overload situation occurs. On another hand, the effect of the subdivision of the coil block into multiple layers, as shown in Figure 14 and Figure 15, on values accuracy is investigated.
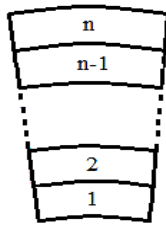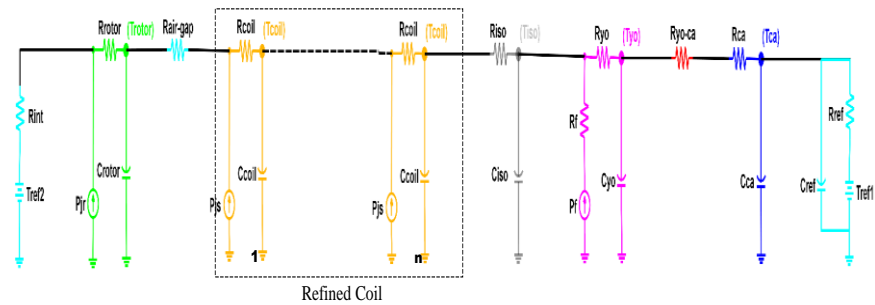

Figure 14. Coil's block subdivision

Figure 15. 1D thermal model with refined coil block

Using the model of Figure 15, the evolution of coil's temperature is carried out in the case of an overload: a short-circuit under nominal voltage with an armature current equal to ten times the nominal one and corresponding to: iron losses (26.5 W), stator copper losses (7260 W) and rotor copper losses (182 W). Moreover, simulations are conducted for a number coil's blocks equal to: 1, 4, 8, 16 and 24, respectively, as illustrated in Figure 16 and summarized in Table 8. Furthermore, a FE calculation is performed in order to validate lumped-circuit results, Figure 17.

Analyzing obtained results, we can notice that:
a. The accuracy of the lumped-circuit follows the increase of the number of coil blocks, despite an increase of simulation time. For that, a compromise should be always found between calculation time and tolerated error.
b. For all considered coil blocks numbers, the error does not exceed 7%. Thus, we judge not necessary to refine the model of Figure 3 and to assign only one block to the coil as the rest of motor components.
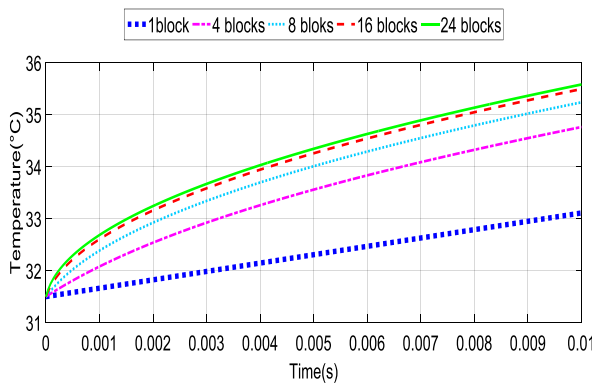

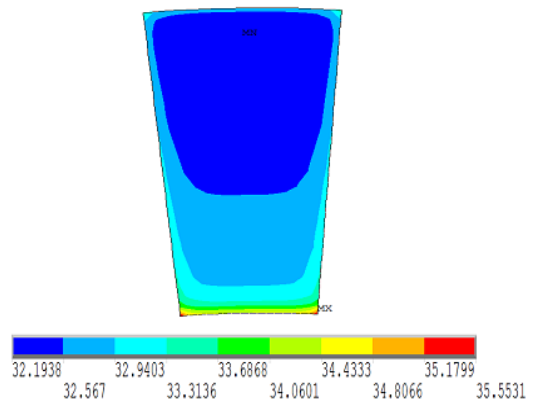Figure 16. Evolutions of the coil temperatures under overload (1D thermal results)

Figure 17. Temperature distribution in the coil at t=0.01

Table 8. Coil temperature at 0.01 s

Number of divisions	1D					EF
	1	4	8	16	24	
Coil temperature (°C)	33.1	34.76	35.23	35.49	35.58	35.55
Percentage error %	6.89	2.22	0.9	0.16	0.08	

5.   CONCLUSION

Electrical machines performances are strongly affected by the thermal states of their components. Thus, the development of tool giving real time information about the temperatures of the device's elements is

a recommended solution, permitting an appropriate control (in normal regimes) and also to predict and avoid damages (in overload cases). Thermal models based on lumped parameters are known by their accuracy, but several of them focus only stator parts. Besides, some model didn't provide the optimal accuracy and rapidity. The originality of this paper consists of the development of a generic refined model giving thermal state of all parts of the machine, along all operation regimes. A lumped-circuit was proposed and validated, through a first study, at no-load and under load regimes. Indeed, All performed tests proved a high satisfactory accuracy level between thermal states of the induction motor obtained through experimental measurement and carried out using the established models (lumped-circuit and FE model), with an error less than 2.7%. Consequently, both models (lumped and FE) were adopted to predict thermal state of the motor in overload operation regime. A short-circuit situation, under nominal voltage and ten times the nominal current, was considered. It has been found that, for all considered coil blocks numbers, the error does not exceed 7%. Thus, in order to avoid the increase of simulation time with no significant improvement of the accuracy, it is not necessary to refine the model and only one block will be assigned to the coil as the rest of motor components. To exploit the developed model, and based on registered progress in software tools, authors are actually working on the development of an advanced platform intended for a control of an electrical machine control integrating a real-time thermal module telling about the thermal state of the machine-converter association.

REFERENCES

[1] Abdelaziz Beddiaf, Fouad Kerrour and Salah Kemouche, "A Numerical Model of Joule Heating in Piezoresistive Pressure Sensors," *International Journal of Electrical and Computer Engineering (IJECE),* vol. 6, pp. 1223-1232, 2016.

[2] Alex Borisevich, "Numerical Method for Power Losses Minimization of Vector-Controlled Induction Motor," *International Journal of Power Electronics and Drive System (IJPEDS),* vol. 6, pp. 486-497, 2015.

[3] Joris Lemmens*, et al.*, "Optimal Control of Traction Motor Drives under Electro-Thermal Constraints," *IEEE Journal of Emerging and Selected Topics in Power Electronics,* vol. 2, pp. 249-263, June 2014.

[4] Jer-Huan Jang, Han-Chieh Chiu, Wei-Mon Yan, M.C.Tsai and Pin-Yuan Wang, "Numerical study on electromagnetics and thermal cooling of a switched reluctance motor," *Elsevier Case Studies in Thermal Engineering,* vol. 6, pp. 16-71, 2015.

[5] P.M.Lindh*, et al.*, "Multidiscplinary Design of a Permanent Magnet Traction Motor for à Hybrid Bus Taking into account the Load Cycle ," *IEEE Transactions on Industrial Electronics,* vol. 63, pp. 3397-3408, June 2016.

[6] Liu Chao*, Ruan Jiangjum, Li Lingyan, Wang Shanshan*, "Study on Temperature Rise of Dry-Type Transformer in Different Cooling Conditions with FEM," *TELKOMNIKA Indonesian Journal of Electrical Engineering,* vol. 12, pp. 7578-7584, November 2014.

[7] Sang-Taek Lee, Hee-Jun Kim, Ju-hee Cho, Daesuk Joo and Dae-kyong Kim, "Thermal Analysis of Interior Permanent-Magnet Synchronous Motor by Electromagnetic Field-Thermal Linked Analysis," *J Electr Eng Technol,* vol. 7, pp. 905-910, 2012.

[8] M.Polikarpova*, et al.*, "Hybrid Cooling Method of Axial-Flux Permanent-Magnet Machines for Vehicle Applications," *IEEE Transactions on Industrial Electronics,* vol. 62, pp. 7382-7390, Dec 2015.

[9] S. C. Mukhopadhyaya and S. K. Pal, "Temperatue analysis of induction motors using a hybrid thermal model with distributed heat sources," *Journal of Applied Physics,* vol. 83, pp. 6368-6370, 1998.

[10] Dave STATON and Livio SUSNJIC, "Induction Motors Thermal Analysis," *Strjarstvo,* vol. 6, pp. 623-631, 2009.

[11] Moez Ayadi, Hana Kebaili, Mohamed Amine Fakhfakh and Rafik Neji, "Simplified Thermal Model of a Radial Flux Motor for Electric Vehicle Application," *Journal of Asian Electric Vehicles,* vol. 8, pp. 1433-1439, 2010.

[12] Shen Yanhua and Jin Chun, "Thermal Behavior of PM in wheel Motor used in Off-road Motor Driven Truck," *Elsevier Procedia Engineering,* vol. 23, pp. 222-228, 2011.

[13] W. Habra*, et al.*, "A New Methodology for Extraction of Dynamic Compact Thermal Models," in *THERMINIC 2007, Sep 2007, Budapest, Hungary. EDA Publishing*, 2007, pp. 141-144.

[14] M. Ayadi, M. A. Fakhfakh, M.Ghariani and R. Neji, "Developing an Equivalent Thermal Model For Discrete Diode Packages," *Elsevier international Journal of Thermal Sciences,* vol. 50, pp. 1484-1491, 2011.

[15] Joris lemmens *et al.*, "Dynamic DC-link Voltage Adaptation for Thermal Management of Traction Drives," 2013 IEEE *Energy Conversion Congress and Exposition (ECCE),* pp. 180-187, 2013.

[16] Sihem Bouguezzi, Moez Ayadi and Moez Ghariani, "Developing a simple analitical thermal model for discrete semiconductor in operating condition," *Elsevier Applied Thermal Engineering,* vol. 100, pp. 155-169, 2016.

[17] Mohand Laid IDOUGHI, "Extraction de modéles thermique simplifies des machines électriques à partir de d'un calcul du champ de températures," *Phd. Thesis,* PARIS-SUD University, Paris, France, 2011.

[18] Xiaofeng Ding, Madhur Bhattachary and Chris Mi, "Simplified Thermal Model of PM Motors in Hybrid Vehicle Applications Taking into Account Eddy Current Loss in Magnets" *Journal of Asian Electric Vehicles,* vol. 8, pp. 1337-1343, 2010.

[19] G. J. Li*, et al.*, "Comparative Studies Between Classical and Mututually Coupled Switched Reluctance Motors Using Thermal-Electrmagnetics Analysis for Driving Cycles," *IEEE Transactions on Magnetics,* vol. 47, pp. 839-847, April 2011.